Biogeosciences

Pumping methane out of aquatic sediments – ebullition forcing mechanisms in an impounded river

A. Maeck[1]**, H. Hofmann**[2]**, and A. Lorke**[1]

[1]University of Koblenz-Landau, Institute for Environmental Sciences, Fortstr. 7, 76829 Landau, Germany
[2]University of Konstanz, Limnological Institute, Mainaustr. 252, 78464 Konstanz, Germany

Correspondence to: A. Maeck (maeck@uni-landau.de)

Abstract. Freshwater systems contribute significantly to the global atmospheric methane budget. A large fraction of the methane emitted from freshwaters is transported via ebullition. However, due to its strong variability in space and time, accurate measurements of ebullition rates are difficult; hence, the uncertainty regarding its contribution to global budgets is large. Here, we analyze measurements made by continuously recording automated bubble traps in an impounded river in central Europe and investigate the mechanisms affecting the temporal dynamics of bubble release from cohesive sediments. Our results show that the main triggers of bubble release were pressure changes, originating from the passage of ship lock-induced surges and ship passages. The response to physical forcing was also affected by previous outgassing. Ebullition rates varied strongly over all relevant timescales from minutes to days; therefore, representative ebullition estimates could only be inferred with continuous sampling over long periods. Since ebullition was found to be episodic, short-term measurement periods of a few hours or days will likely underestimate ebullition rates. Our results thus indicate that flux estimates could be grossly underestimated (by up to ~ 50 %) if the correct temporal resolution is not used during data collection.

1 Introduction

Methane (CH_4) is regarded as the second-most important anthropogenic greenhouse gas, with global emission rates between 500 and 600 Tg yr^{-1} (Forster et al., 2007). The contribution of freshwater systems is estimated to be around 103 Tg CH_4 yr^{-1}, of which over 53 % is emitted via gas bubbles (Bastviken et al., 2011).

Gas bubbles released from anoxic freshwater sediments often consist of a large proportion of CH_4 (Baulch et al., 2011). In these sediments where alternative electron acceptors, e.g., nitrate or sulfate, are lacking or depleted and degradable organic carbon (C_{org}) is available, CH_4 is produced by organisms of the domain archaea. The rate of production depends on the amount and quality of C_{org} and temperature (Duc et al., 2010; Liikanen and Martikainen, 2003; Segers, 1998; Sobek et al., 2012). Produced CH_4 can dissolve into the porewater, and thus continuous production in combination with low efflux rates can lead to high concentrations of CH_4 within the porewater (Maeck et al., 2013). If the partial pressure of all dissolved gases in the porewater exceeds the ambient pressure and the surface tension of water, free gas is formed. Due to ongoing production of CH_4, bubbles within the sediments grow and form fractures or disc-shaped cavities (Boudreau et al., 2005; Johnson et al., 2002).

The mode of transport of CH_4 from the sediments to the atmosphere has important implications. Transport via diffusion is relatively slow and CH_4 oxidizing bacteria can oxidize a large proportion of the produced CH_4 (Segers 1998). Surface waves are known to increase the near-bottom current velocities and to cause sediment resuspension in the shallow littoral, which triggers and accelerates the diffusive flux of CH_4 across the sediment–water interface (Hofmann et al., 2010). However, if free gas in the form of rising bubbles is released, the transport is too fast for microbial oxidation at the sediment–water interface and a larger fraction of the initial CH_4 reaches the atmosphere (Kiene, 1991). If bubbles migrate slowly through the upper layer of the sediment,

where O_2, NO_3^- or SO_4^{2-} is present, a larger fraction of the free CH_4 gas can re-dissolve and be oxidized (Venkiteswaran et al., 2013). In terms of atmospheric emissions, physical and chemical parameters like the water depth, bubble size and the concentration of CH_4 in the ambient water determine what fraction of the initially released CH_4 reaches the atmosphere (Leifer and Patro, 2002; McGinnis et al., 2006). Although it varies with depth and environmental conditions, the fate of rising CH_4 bubbles in the water column is well understood (Leifer and Patro, 2002; McGinnis et al., 2006), studies investigating the mechanisms responsible for the temporal and spatial dynamics of bubble release are rare. The spatial variability of ebullition in impounded rivers was recently shown to correlate strongly with spatial patterns of sedimentation (Maeck et al., 2013). In a large reservoir, DelSontro et al. (2011) found higher ebullitive fluxes in river delta bays compared to non-river bays, which may also point towards sedimentation as the main cause of the spatial distribution of ebullition. To build on this work, we focus the current study on the temporal variability of ebullition in greater detail at a site known for spatially variable ebullition in order to investigate its underlying processes better.

Most studies suggest that ebullition occurs episodically (Coulthard et al., 2009; Goodrich et al., 2011; Varadharajan and Hemond, 2012; Wik et al., 2013). The episodic pattern may be related to a complex interplay between bubble buoyancy and sediment mechanics. Numerical modeling suggests that bubble rise within the sediment is driven by dilating conduits or rise tracts ("transport pipes") that facilitate gas transport due to their higher flow conductance (Scandella et al., 2011). The mechanism dilating the conduits and therefore controlling the temporal pattern of bubble release is assumed to be hydrostatic pressure (Scandella et al., 2011). Another study showed that shear stress at the sediment–water interface is correlated with ebullition rates (Joyce and Jewell, 2003). The origin of hydrostatic pressure or shear-stress changes can be various physical phenomena, e.g., waves or water level changes, which are further denoted as forcing mechanisms. Studies showed that forcing mechanisms affecting ebullition rates can be air pressure changes, tides, wind or water level changes (Chanton et al., 1989; Joyce and Jewell, 2003; Varadharajan and Hemond, 2012). The timescales on which forcing mechanisms trigger ebullition are variable, e.g., surface waves act on timescales of seconds to minutes, while air pressure or water level changes can vary significantly on scales of days to weeks, and since ebullition rates are directly affected by the temporal dynamics of forcing mechanisms, we hypothesize that both are strongly correlated.

Within this study, we present continuous ebullition rate measurements made in an impounded river in central Europe, which is known for its highly variable hydrostatic pressure due to ship lock-induced surges (Maeck and Lorke, 2013). We used automatic bubble traps (ABTs) to measure ebullition rates with a high temporal resolution continuously over a period of five months in an impounded river in central Europe. The data are analyzed in combination with time series of hydrostatic and air pressure (as well as other parameters) to investigate the relationship between forcing mechanisms and gas release in greater detail. The scope of this study is (1) to quantify the temporal variability of ebullition rates in an impounded river, (2) to estimate the relevant timescales of variability, and (3) to identify the corresponding forcing mechanisms. Furthermore, we will use these results to review the potential uncertainties associated with limited sampling periods of ebullition measurements described in the literature.

2   Material and methods

2.1   Study site

Flowing along 246 km through France and southwest Germany, the River Saar discharges a watershed of 7.363 km^2 in central Europe. The mean discharge at the Fremersdorf gauging station (48 km) is 75 m^3 s^{-1}. During the period from January 2010 to February 2013, the discharge often ranged between 20 and 40 m^{-3} s^{-1} ($\sim$ 60 % of all days), but peaks up to 675 m^{-3} s^{-1} also occurred. The German part of the river (the lower 96 km) was impounded between 1976 and 2000 for navigation purposes. Therefore the river bed was channelized over long distances and six dams with ship locks and hydropower plants were built.

The damming of the river led to increased water depths (up to 11 m), prolonged water residence times (Schöl, 2006), and strong sedimentation upstream of the dams, where the flow velocity is reduced (Maeck et al., 2013). To maintain cargo shipping, the riverbed is dredged on demand to ensure a minimum depth of 4 m within the shipping channel. However, sediment layers of up to 5 m thickness exist in zones outside of the shipping channel, e.g., at the inner bending of river meanders. A longitudinal study along the entire River Saar showed that most of the CH_4 emissions (> 90 %) originate from the zones of high sedimentation that are located upstream of the dams (Maeck et al., 2013). These zones exhibit a more reservoir-like than riverine character, with reduced flow velocities, thermal stratification during periods of high solar radiation, and higher average water depths (Becker et al., 2010).

For this study, we measured ebullition and pressure from 16 October 2012 to 6 March 2013 at three sites approximately 1 to 2 km upstream of the Serrig Dam (Fig. 1). This river stretch is characterized by intensive sediment accumulation (1 to 5 m within the periods of 1993 and 2010, Fig. 1b) and strong methane ebullition (Maeck et al., 2013).

The water level in the Serrig impoundment is regulated by the Serrig Dam, but water import or export from ship lock chambers induces strong short-term discharge changes, which propagate as surges (Maeck and Lorke, 2013). Surges
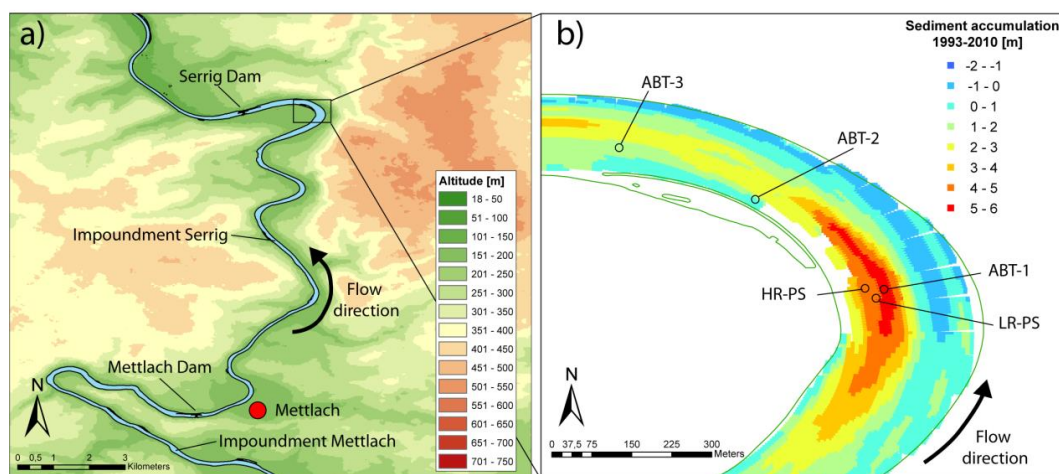
Figure 1. Location of the sampling sites. **(a)** Topographic map of the Serrig impoundment (49.576° N, 6.600° E), which is enclosed by the upper dam in Mettlach and the lower dam in Serrig. The sampling sites are located ∼ 1 to 2 km upstream of Serrig dam in the inner bending of the river meander. **(b)** Map of the sampling sites showing sediment accumulation within the Serrig impoundment (Maeck et al., 2013). The positions of deployment sites for three automatic bubble traps (ABT 1 to 3), the high-resolution pressure sensors (HR-PS) and the low-resolution pressure sensor (LR-PS) are indicated.

are gravity waves, either shaped as a solitary wave crest (positive surge) or trough (negative surge), which propagate along the entire basin, are reflected at the next dam and propagate backwards (USACE, 1949). Superposition of multiple surges led to water level fluctuations of up to ∼ 30 cm, which is comparable to long-term reservoir storage changes (Maeck and Lorke, 2013). Associated with water level changes during the passage of surges are changes in the mean flow velocity, which can create flow reversals (Maeck and Lorke, 2013).

2.2 Measurement of ebullition rates

Ebullition was measured continuously using three ABTs at sites with a net sediment accumulation rate of 0.29, 0.07 and 0.1 m yr^{-1} and a water depth of 4, 2 and 2.7 m, respectively (net sediment accumulation rates measured between 1993 and 2010; Fig. 1b, Maeck et al., 2013).

An ABT consists of an inverted polypropylene funnel with a diameter of 1 m, a cylindrical gas capture container (diameter 23 or 29 mm), a differential pressure sensor (PD-9/0,1 bar FS, Keller AG) and a custom-made electronic unit (data logger and regulation device for venting the gas capture container, Fig. 2b). The entire ABT was deployed submerged so that rising gas bubbles within the water column were collected by the funnel and the gas accumulates in the cylindrical container. To install the ABTs at a specific location, the ABTs were connected with two 9 m ropes to anchor weights. The weights were placed in the distance so that the sediment below the ABTs was not disturbed. The deployment of one weight upstream and one weight downstream ensured that the ABTs were always in the same position.

The water level within the gas-capturing container was monitored at an interval of 5 s using the differential pressure between the inside of the container and the outside. The gas-capturing container was automatically emptied as soon as the captured gas reached the storage capacity. Therefore, the electronic unit opens a solenoid valve that vents the system and a new measurement cycle starts.

The amount of gas was calculated using the ideal gas law

$$n = \frac{p_i \times (\pi \times r^2 \times H)}{R \times T}, \tag{1}$$

where n denotes the number of moles [mol], p_i the partial pressure of CH_4 [Pa], r the radius of the cylindrical gas container [m], H the measured fill height [m], R the universal gas constant [m^3 Pa K^{-1} mol^{-1}] and T the temperature [K]. The fill height describes the water level within the gas capturing cylinder and was inferred by measuring the differential pressure between the inside and outside of the cylinder as described in Varadharajan et al. (2010). Temperature measurements were performed using an RBR TR-1060 sensor with an accuracy of ± 0.008 °C attached to the ABTs. The partial pressure was calculated as the product of absolute pressure (10^5 Pa or 1 bar) and the mean mole fraction of CH_4 in the gas bubble (0.80, see results section).

By using the number of moles of CH_4 (n), the base area of the funnel A [m], and the timestamps of the data logger (t_{i+1} and t_i) [d], the ebullition rate E [mol m^{-2} d^{-1}] was estimated as

$$E = \frac{n}{A \times (t_{i+1} - t_i)}. \tag{2}$$

Every four weeks, the system was recovered for cleaning, data download, calibration and battery replacement. For
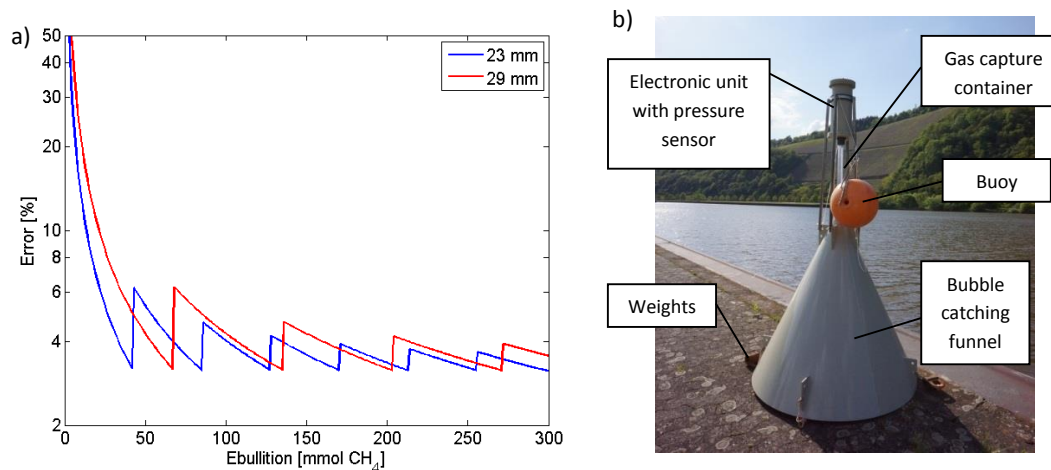
Figure 2. (a) Error in the volume determination in relation to the captured gas for two different diameters of the gas capture container (23 and 29 mm). The saw-like steps in the curve result from venting of the system and the start of a new filling cycle. Since for every cycle two additional differential pressure sensor readings are necessary, error increases temporarily due to flushing. **(b)** Automated bubble trap device. The instrument operates submerged and catches rising bubbles. The captured gas is stored in the cylindrical gas capture container and the fill height of the container is measured via differential pressure with the electronic unit.

calibration of the differential pressure sensor the capture container of each ABT was submersed in a glass cylinder and air was injected manually to achieve a specific fill height measured visually with an attached scale bar. An average differential pressure sensor reading was recorded for five different fill heights and linear regression analysis was used to determine the corresponding calibration coefficients. The goodness-of-fit R^2 value was always > 0.98. A temperature correction was applied electronically within the electronic unit.

The nominal accuracy of the differential pressure sensor given by the manufacturer is 50 Pa, which corresponds to a water level of approximately 0.5 cm. Since absolute accuracy increases linearly with the difference in water level within the container at two points in time, the accuracy increases with ebullition rate. However, each system venting decreases the accuracy since two additional measurements are required for each venting; one at the maximum fill level and one base value, when the system is emptied completely (Fig. 2). Therefore, the accuracy is non-linear over the entire range of measured volumes but for gas volumes exceeding 410 (23 mm pipe diameter) and 640 ml (29 mm pipe diameter) corresponding to 13.5 and 21.3 mmol CH_4 (at 20 °C, 1 bar and assuming 80 % CH_4 content in the captured gas, respectively) it is always below 10 %. Thus, high ebullition rates can be quantified with the ABT over long periods with an error of less than 10 %.

2.3 Pressure measurements

Hourly mean air pressure data were obtained from the German Weather Service (Trier–Petrisberg station 49.7492° N,

6.6592° E), located approximately 20 km north of the sampling sites.

We deployed a pressure and temperature sensor (LR-PS, RBR-2050, RBR Ltd., Canada) on the riverbed close to the ABT-1 automatic bubble trap (Fig. 1b) during the study period from 16 October 2012 to 6 March 2013. Data was recorded at an interval of 5 s. The accuracy of the pressure sensor is 0.25 mbar at a resolution of 0.05 mbar, while the accuracy of the temperature sensor is ± 0.008 °C.

To characterize the surface wave field, a custom-made high-resolution pressure sensor (HR-PS) (Hofmann et al., 2008a) was deployed in the vicinity of ABT-1 at a height of ∼ 1 m above the riverbed at ∼ 1.8 m water depth (Fig. 1b). Data was recorded at a frequency of 16 Hz.

2.4 Concentration of CH_4 within the bubbles

To determine the concentration of CH_4 within gas bubbles, an anchor weight of > 10 kg was used to disturb the sediment surface and release bubbles in a distance of approximately 5 to 8 m from the ABTs. They were caught immediately in the first 1.5 m of their rise with an inverted funnel (diameter 0.6 m) equipped with a 1.5 l gas container. The gas was transferred with a syringe to triplicate brine-filled (saturated NaCl-solution) 20 ml headspace vials sealed with a butyl-rubber stopper. An injected needle allowed brine to flow out while the gas was transferred from the syringe into the vial. Approximately 5 ml of brine remained in the vials as a diffusion barrier to minimize leakage when the vials were stored upside down. CH_4 concentration in the headspace was measured in the lab using gas chromatography (Varian, CP-3800, flame-ionization detector). Therefore, a packed column (Porapack[TM]) was used at a temperature of 60 °C and

a flow rate of the N2-carrier gas of 8 ml min^{-1}. Calibrations were established by using commercial CH$_4$ standards (Linde Gas, Germany) for every set of measurements separately.

2.5 Analysis

2.5.1 Characterizing ebullition rates

Since the ebullition rates showed non-Gaussian distributions, we used the median and percentiles to express ebullition rates. For the comparison between daytime (7 am to 7 pm) and nighttime (7 pm to 7 am) ebullition rates, the average hourly flux rates per day during the day and night were calculated. The difference between day- and night-time ebullition rates was analyzed using a Wilcoxon ranksum test.

2.5.2 Estimating the error of the monthly mean ebullition rate by subsampling

Our data set consists of continuous (5 s interval) measurements of ebullition rates from 16 October 2012 to 7 March 2013. Subsets of 1 to 720 consecutive hours were drawn from the total data set. The mean ebullition rate of the subset $\overline{E_{\text{subset}}}$ was compared with the mean ebullition rate of the surrounding 30 days $\overline{E_{30\,\text{days}}}$ including the subset (e.g., for a subset of 24 hours, the 14.5 days before, the 24-hour subset and the 14.5 days after the subset were used), where D denotes the deviation of the subset from the monthly mean in %

$$D = \frac{\overline{E_{\text{subset}}}}{\overline{E_{30\,\text{days}}}} \times 100\,\%. \tag{3}$$

The subsets were shifted through the entire data set so that the results of many subset deviations were used to calculate the 10th, 50th and 90th percentile deviations from the 30-day mean ebullition rate.

2.5.3 Frequency spectrum

To determine the relevant timescales of pressure variability and ebullition we estimated power spectral density using Welch's method with a Hamming window and a 50 % overlap (Emery and Thomson, 2001). In the ebullition data set, the instantaneous ebullition rate with a sampling interval of 5 s was used after exclusion of outliers (> 1000 times the average ebullition rate). The window size for the ebullition rate spectrum was 2^{14} measurements for periods < 24 h and 2^{20} for periods > 24 h to combine both spectra with a composite spectrum. For the LR-PS and HR-PS (pressure sensor) data, 2^{19} samples were used.

2.5.4 Characterizing low- and high-pressure variability periods

The contributions of surface waves and surges to the total variability of hydrostatic pressure were discriminated using a high-pass filter (fifth-order Butterworth) with a cut-off frequency corresponding to a 6 h period. By using a running standard deviation (RSTD, window size 30 min) on the high-frequency pressure signal, periods of high- and low-pressure variability were identified. The pressure data were divided into 1 h windows and the mean of the RSTD of the window was compared to the mean RSTD of the entire time series. Windows with an average RSTD below the RSTD of the entire time series were categorized as "low-variability periods", while periods with an RSTD above the mean RSTD were designated as "high-variability periods".

2.5.5 Determining trigger mechanisms for ebullition

The 5-minute resolution time series of ebullition was analyzed in combination with hydrostatic pressure records. All large ebullition events, defined as when all three ABTs had values exceeding 56 mmol CH$_4$ m^{-2} d^{-1} (corresponding to $\sim$ 1 g CH$_4$ m^{-2} d^{-1}), were selected and the corresponding time period in the hydrostatic pressure data was then categorized according to the following: (1) negative surges, (2) positive surges, (3) decreasing water level, (4) ship passages or (5) without changes.

3 Results

3.1 Physical environment

During the study period from 16 October 2012 to 6 March 2013, the average daily discharge ranged from 18.5 to 405 m^3 s^{-1} (Fremersdorf gauging station), with an average of 109 m^3 s^{-1} and a median of 63 m^3 s^{-1}. Over 50 % of all days, the discharge was below 65 m^3 s^{-1}. Three major flood peaks occurred from 2 to 13 November, 14 December to 8 January, and 28 January to 14 February (Fig. 3). Water temperature ranged between 2.8 °C and 13.5 °C (Fig. 3). From 16 to 27 October, diurnal thermal stratification occurred. The water column was well mixed during the rest of the study period.

The total pressure at the sediment surface is the sum of atmospheric pressure at the water surface and gravitational pressure imposed by the water column, which is controlled by the water level. Both parts contributed with similar magnitudes to the observed variability of total pressure at the sediment surface (76 % of the total variation is contributed by hydrostatic and 24 % by atmospheric pressure changes), but show distinct differences in the spectral distribution of variance (Fig. 4). While both air pressure and water level varied on timescales of days to weeks, the hydrostatic pressure also showed strong variability on the timescale of minutes to hours (Fig. 3), which is in most cases the result of ship lock-induced surges (the peaks in Fig. 4 at 15 min, 32 min and 65 min) (Maeck and Lorke, 2013). Since the water level is regulated by the Serrig Dam, maximum changes in water level, even during high-discharge periods, were below
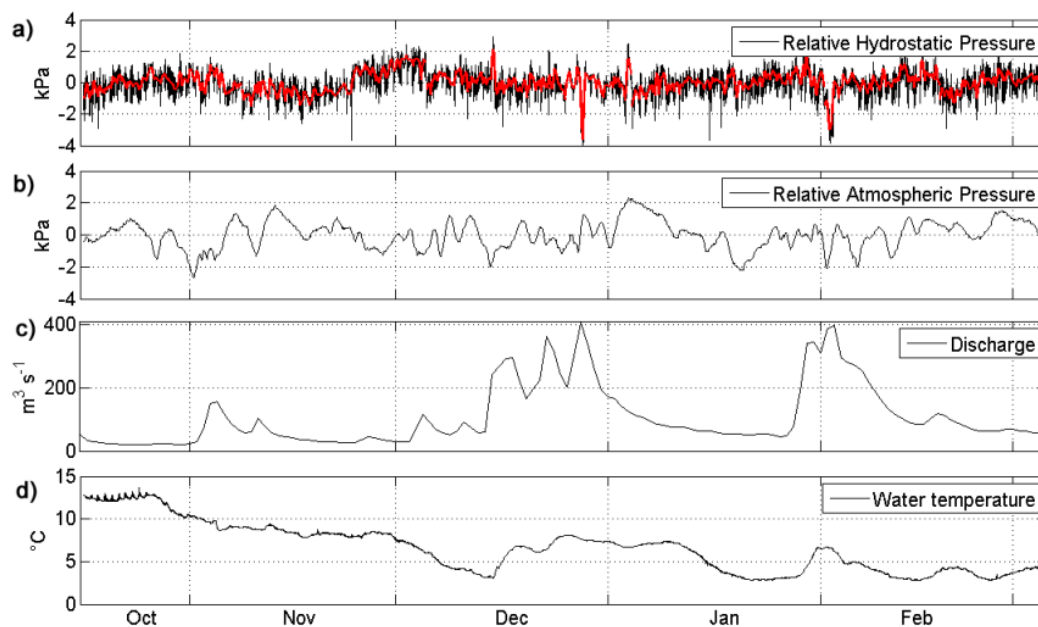
Figure 3. (a) Relative hydrostatic (original data in black, low-frequency filtered in red), **(b)** atmospheric pressure, **(c)** discharge and **(d)** water temperature between 16 October 2012 and 6 March 2013.

0.74 m, while the standard deviation of the water level was 0.07 m (Fig. 3).

Analysis of the high-pass filtered hydrostatic pressure signal of the LR-PS allowed one to distinguish periods with high and low pressure variability. The high-variability periods were characterized by intensive ship locking activity that induced multiple surges (Maeck and Lorke, 2013), and corresponding passages of ships were observed. The passage of a surge is characterized by a defined wave crest or trough over a period of $\sim$ 12 min, while the passage of a ship often showed a strong (up to 30 cm of water level) but short (< 1 min) decrease in pressure in the LR-PS signal. In the HR-PS measurements, ship waves could be discriminated from wind-induced surface waves by their short duration and due to their higher maximum wave amplitude. We chose a threshold of 2 cm for separation. Ship waves showed on average a maximum wave height of 4.2 cm; however, they often reached maximum wave heights between 10 and 20 cm.

3.2 Characterization of ebullition

Deliberately released gas bubbles had CH_4 volume concentrations between 48.6 % and 92.1 % with a mean of 80.5 %. For the conversion of the volume measurements with the ABTs to the ebullition rate, a concentration of 80 % CH_4 was used (Table 1). Gas concentrations of naturally released bubbles are reported to vary strongly, but since we focus on the temporal dynamics in ebullition, we used the average concentration of deliberately released bubbles for the flux estimates.

We observed high variability in the ebullitive flux on all temporal scales, ranging from minutes to days (Fig. 5). The daily ebullition rate ranged from 0 up to 240, 48 and 147 mmol CH_4 m^{-2} d^{-1} for ABT-1, ABT-2 and ABT-3, respectively. The median daily ebullition rate for the entire sampling period was 22.4 (8.8/48.3, values represent the 25th and 75th percentiles), 3.5 (0.6/8.0) and 9.1 (3.5/16.8) mmol CH_4 m^{-2} d^{-1}, at ABT-1, ABT-2 and ABT-3, respectively. From October to the end of January, the mean monthly ebullition rate showed no trend, while in February, the ebullition rate increased strongly for ABT-1 and ABT-3.

A significant difference in the ebullition rate between day- and night-time could be observed for all three ABTs (Wilcoxon test, p values are all below 0.05). On average, the daytime ebullition rates were 62 %, 42 % and 11 % higher compared to the nighttime ebullition rates for ABT-1, ABT-2 and ABT-3, respectively.

Most of the variability of the ebullition rate occurred on short timescales below one day (Fig. 4), e.g., the 5 min ebullition rate varied much more strongly compared to the 1 h or 1 d ebullition rate (Fig. 5). The frequency distribution of spectral variance (Fig. 4) shows that most variability is associated with timescales between 1 min and 2 hr, but distinct peaks at higher frequencies with corresponding time periods of < 1 min were also observed. These high-frequency spectral peaks, however, are potentially measurement artifacts caused, for example, by surface wave-induced oscillations of the ABT mooring as well as by the discrete nature of ebullition. Longer-term variability (e.g., day-to-day changes in ebullition rates) exceeding one order of magnitude also
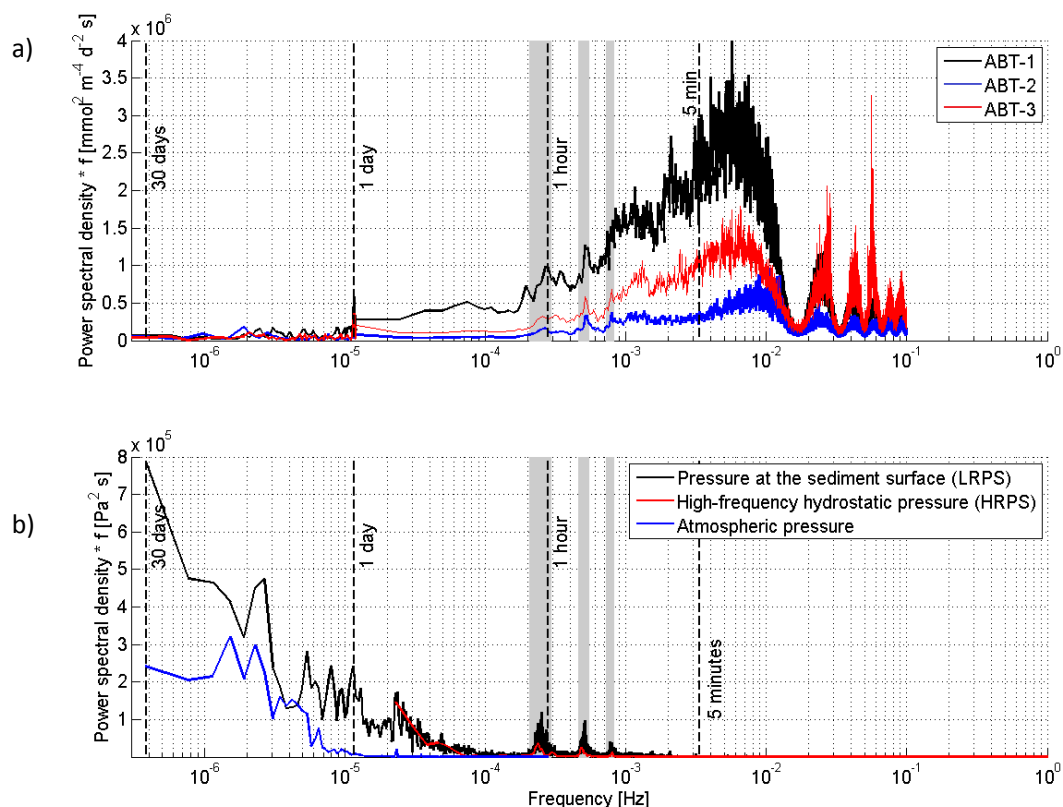
Figure 4. Variance-preserving power spectra of ebullition rates **(a)** and hydrostatic (LR-PS and HR-PS) and atmospheric pressure in **(b)**. Peaks at 15 min, 30 min and 1 h are marked in grey and caused by ship lock-induced surges.

Table 1. Monthly mean $\pm$ SD and overall mean $\pm$ SD concentrations of CH_4 in deliberately released and captured bubbles of the three automated bubble traps (ABTs) during the entire sampling period.

	Nov	Dec	Jan	Feb	Mar	Mean $\pm$ SD per ABT
	[% CH_4]	[% CH_4]	[% CH_4]	[% CH_4]	[% CH_4]	[% CH_4]
ABT-1	89.8	81.1	48.6	71.1	89.5	76.0 $\pm$ 17.1
ABT-2	89.2	80.9	76.6	78.0	88.5	82.6 $\pm$ 5.9
ABT-3	89.5	84.2	72.8	75.0	92.1	82.7 $\pm$ 8.6
Monthly mean $\pm$ SD	89.5 $\pm$ 0.3	82.1 $\pm$ 1.8	66.0 $\pm$ 15.2	74.7 $\pm$ 3.5	90.0 $\pm$ 1.9	80.5 $\pm$ 10.2

occurred frequently. Therefore, the best approach to achieving a representative estimate of the monthly mean ebullition rate is to use longer measurement periods for the calculation. Figure 6 shows how the range between the 10th and 90th percentiles of the subset mean ebullition rate is largest for sampling durations of only several hours and decreases with increasing measurement periods. Ultimately, there was an 80 % chance of estimating the 30-day mean ebullition rate with a precision of $\pm$ 50 % after measurements of consecutive 303, 375 or 280 hr for ABT-1, ABT-2 and ABT-3, respectively.

Ebullition occurred episodically, often in bursts of several bubbles entering the bubble trap indicated by the observation that the volume measured every 5 s often exceeded the volume of a typical bubble having a 5 mm diameter and a volume of $\sim$ 0.5 ml (McGinnis et al., 2006). Not all but many bursts were synchronized between all three ABTs (Fig. 7). The cross-correlation between ABTs shows a distinct maximum at zero lag, which indicates that a major portion of ebullition events are synchronized. Secondary small peaks were observed at a $\pm$ 1 h time lag, which corresponds to the re-occurrence of ship lock-induced surges after propagation along the entire impoundment, reflection and backward propagation (Maeck and Lorke, 2013).

3.3 Mechanisms triggering ebullition

Analysis of all synchronized 5 min ebullition rates where all ABTs measured values exceeding 56 mmol CH_4 m^{-2} d^{-1}
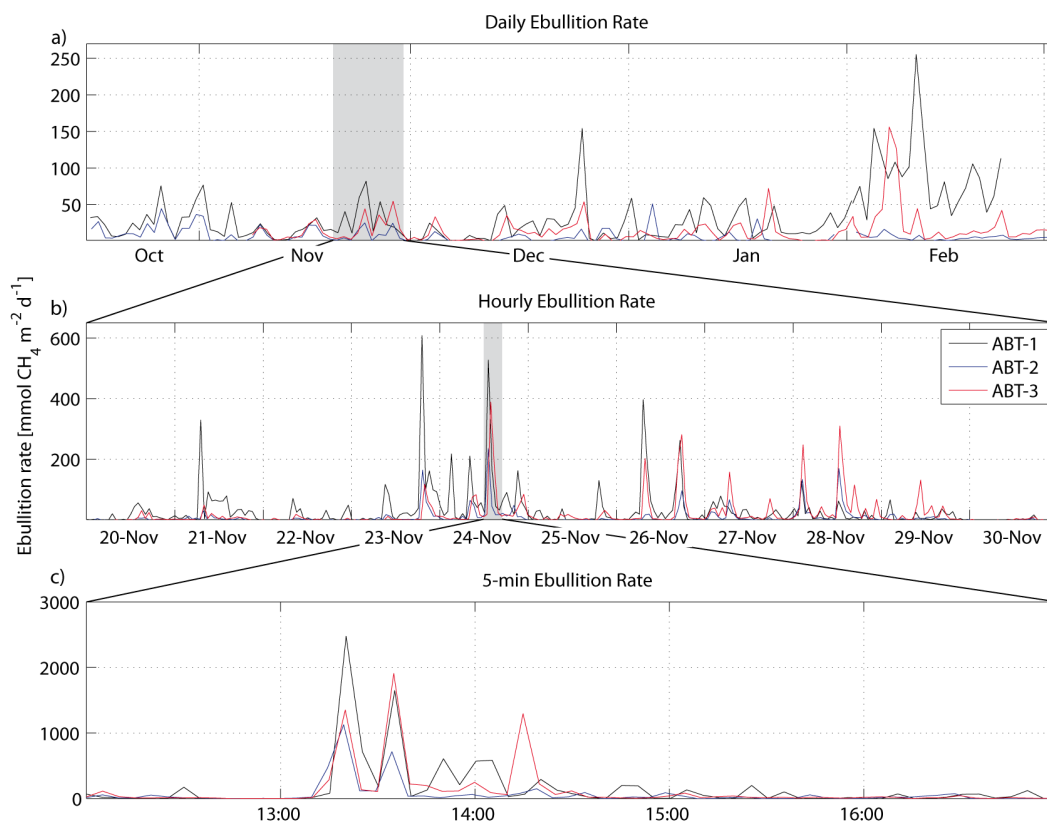
Figure 5. Temporal variability of ebullition rates observed using the three automated bubble traps (ABTs) at different timescales: **(a)** Daily mean ebullition rates for the entire sampling period. **(b)** Hourly mean and **(c)** 5 min mean ebullition rates for selected time periods indicated by the grey bars in **(a)** and **(b)**.

Table 2. Ebullition rates in mmol m^{-2} d^{-1}. All ebullition rates are shown as the median and 25th and 75th percentiles (in brackets). The day- and night-time ebullition rates refer to the hourly measured ebullition rates, while the daily ebullition rate is based on the daily ebullition rate. The N, p values and z values represent the results of a Wilcoxon test comparing day- and night-time ebullition rates.

	ABT-1	ABT-2	ABT-3
Daily ebullition rate	22.4 [8.8–48.3]	3.5 [0.6–8.0]	9.1 [3.5–16.8]
Daytime ebullition rate (7 am–7 pm)	20.4 [10.1–62.2]	1.7 [0.6–7.3]	9.3 [3.6–20.9]
Nighttime ebullition rate (7 pm–7 am)	12.6 [4.4–35.0]	1.2 [0.36–4.6]	3.7 [1.2–12.4]
N, p value, z value	98, < 0.01, 2.76	102, 0.04, 2.06	102, < 0.01, 3.07

(corresponding to $\sim 1\,\mathrm{g\,CH_4\,m^{-2}\,d^{-1}}$) revealed that 59.4 % of all investigated ebullition rates occurred during the passage of a negative ship lock-induced surge (wave trough), 26.4 % during the passage of a ship, 5.7 % during periods of sinking water levels and 7.5 % during times where no pressure change was observed. Only one of the investigated ebullition events (0.9 %) was observed during the passage of a positive surge. The detailed temporal dynamics of ebullition rates in relation to the major forcing mechanisms are exemplified in Fig. 8. The physical forcing of bubble release by surges and ship passages was the major regulator for the tim-

ing of ebullition. However, we also observed examples where no response of ebullition followed these forcing events.

The hydrostatic pressure varied strongly during 46 % of the entire sampling period due to ship lock and ship activity (Maeck and Lorke, 2013), but contributed 61 %, 72 % and 66 % to the total gas flux variability at ABT-1, ABT-2 and ABT-3, respectively. Mean emission rates during high-pressure variability periods (44, 12 and 21 mmol $\mathrm{CH_4\,m^{-2}\,d^{-1}}$), mostly occurring at daytime due to intensive ship activity (Maeck and Lorke, 2013), were two to three times higher than emission rates during low-pressure
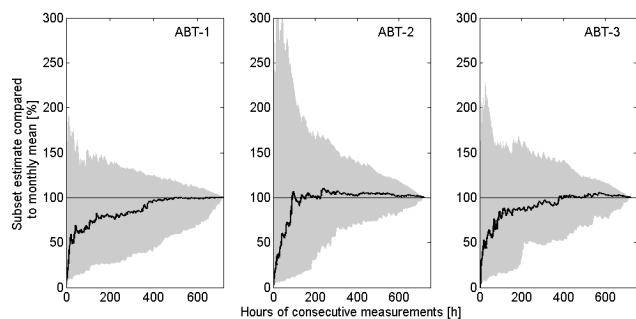
Figure 6. Mean ebullition rates averaged over subsets of varying length representing consecutive measurement periods normalized by the mean ebullition rate observed over a 30-day period centered around the respective subset for the automated bubble traps (ABT 1 to 3) (left to right). The black line shows the median of all subsets and the grey area denotes the 10th and 90th percentiles.

Figure 7. Cross-correlation coefficients of the 5 min ebullition rates versus the time lag of the three ABTs against each other. Peaks at zero lag indicate that both signals are synchronized.

variability periods (22, 4 and 8 mmol CH_4 m^{-2} d^{-1} for ABT-1, ABT-2 and ABT-3, respectively).

4 Discussion

4.1 Variability and magnitude of ebullitive emissions

All sampling sites of this study are characterized by high sediment accumulation and high CH_4 concentrations and ebullitive release, which indicates high production rates of CH_4 (Maeck et al., 2013). The trend that ebullition rates positively correlate with sediment accumulation rates observed by Maeck et al. (2013) also holds true for the long-term measurements presented here. ABT-1 located over a site with the highest sediment accumulation rate (0.29 m yr^{-1}, Fig. 1, determined following Maeck et al., 2013) showed the highest mean ebullition rate, followed by ABT-3 and ABT-2 with sediment accumulation rates of 0.1 and 0.07 m yr^{-1}, respectively. Therefore, the CH_4 production rate per square meter likely differs between the three sites. If CH_4 production rates correlate with sedimentation rates, which is likely, then we observe that the variability in the daily ebullition rate also increased with production rate. However, it is likely that the ebullition variability was a factor in frequent forcing as well as production rate (Fig. 9).

The magnitude of CH_4 ebullition rates measured in the present study are lower compared to the results of Maeck et al. (2013), where the ebullition rate was measured using hydrostatics and correlated with the sediment accumulation rate (22.4 vs. 431, 9.1 vs. 14.4 and 3.5 vs. 8.4 mmol CH_4 m^{-2} d^{-1} for ABT-1, ABT-2 and ABT-3, respectively), which may be the result of differing sediment temperatures. While the data presented here were measured during the winter when temperatures were low, the study by Maeck et al. (2013) was performed in September when water temperatures were higher. However, these current results are higher than total CH_4
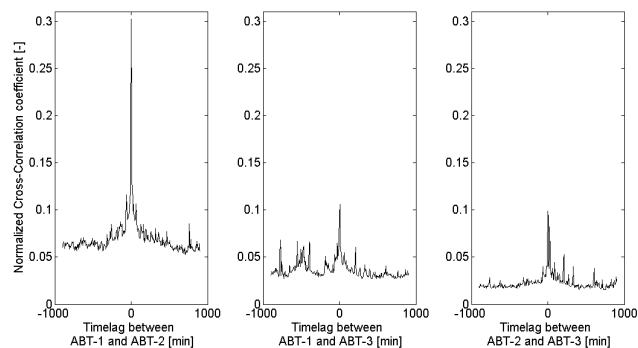
emission rates reported for temperate lakes, rivers or reservoirs (4, 0.9 and 1 mmol CH_4 m^{-2} d^{-1}, respectively) and comparable to emissions of tropical ($< 25°$ latitude) reservoirs (16 mmol CH_4 m^{-2} d^{-1}, Bastviken et al., 2011; Varadharajan and Hemond, 2012), as was also observed in a Swiss hydropower reservoir (DelSontro et al., 2010). The temporal variability of ebullition rates was extremely high, as observed by Varadharajan and Hemond (2012); hence, for reliable measurements of ebullitive emissions the temporal variability must be considered in the planning stages of future studies.

Our results clearly show that ebullition is episodic, occurring in bursts consisting of many bubbles. The reason for this can be two-fold. On the one hand, external forcing (e.g., pressure reduction) can increase the volume of all bubbles within the sediment, from which a portion then has a buoyancy exceeding the strength of the surrounding sediment and starts to rise (Boudreau et al., 2005). On the other hand, as soon as the first bubbles rise, they form conduits or rise tracks that make it easier for other bubbles to follow (Boudreau et al., 2005; Scandella et al., 2011). Besides external forcing, bubbles can also be released by ongoing CH_4 production and continuous bubble growth and rise. This mechanism would lead to unsynchronized ebullition rates between sites and, when averaged over longer timescales, to constant flux rates that will then respond to changes in CH_4 productivity, e.g., due to temperature changes or changes in the amount of organic matter to be mineralized. The results of this study show, however, that anthropogenic mechanical forcing dominates the temporal pattern of ebullition on timescales of days to weeks, not continuous CH_4 production.

During our study period, temperatures in the water column were low and ranged between 3 and 8 °C. However, since CH_4 production occurs mainly within the sediments, the temperature within the sediment is the effective temperature regulating biogeochemical reaction kinetics and therefore CH_4 production. Sediment temperature itself is affected by heat exchange with the overlying water column and with
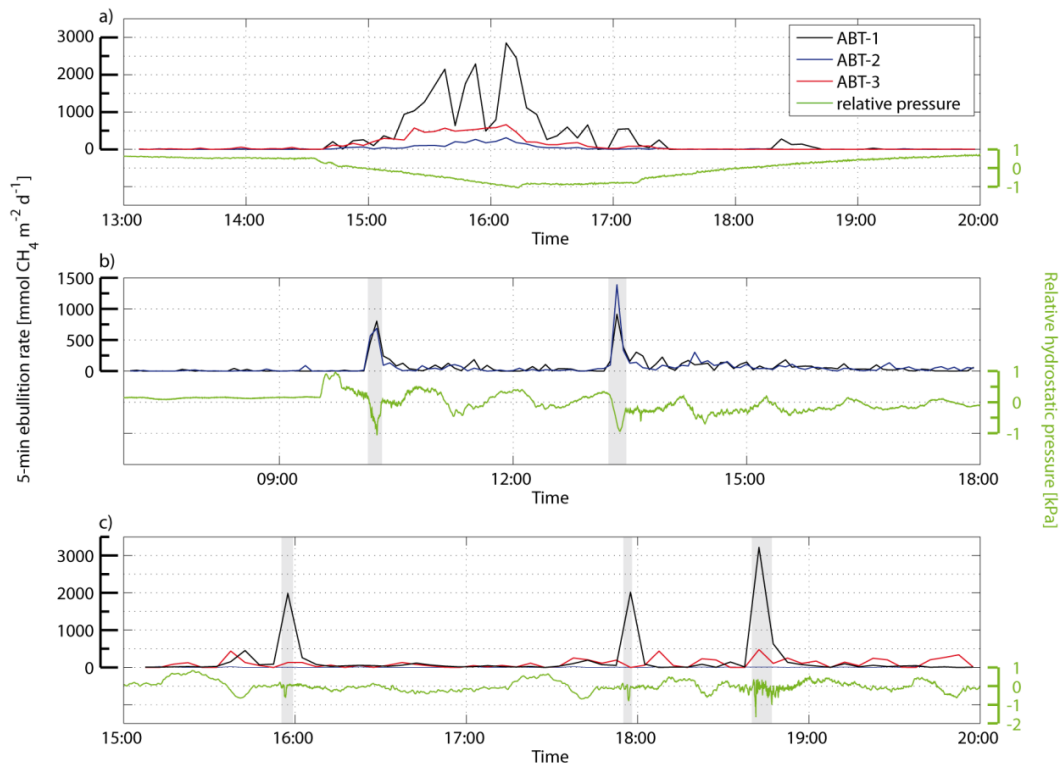
Figure 8. Time series of 5 min ebullition rates and hydrostatic pressure changes. Panel **(a)** shows bubble release during sinking water level within a high-discharge period (25 December 2012). Panel **(b)** shows the relationship between positive and negative (grey shaded) surges and the ebullition rates (31 October 2012), while panel **(c)** highlights ebullition during the corresponding ship passages (grey shaded) (18 February 2013).

the groundwater, and to a lesser extent by microbial heat production associated with the degradation of organic matter (Fang and Stefan, 1996; Fang and Stefan, 1998). Only the top layer of the sediment is strongly affected by heat exchange with the overlying water column and therefore subject to pronounced temperature variations, while the temperature variability decreases with increasing depth (Fang and Stefan, 1998). Since water temperatures were low, we assume that during our study period the production zone of CH_4 was mainly within deeper sediment layers, where the effective temperature for methanogenesis changed only slowly compared to the timescale of forcing mechanisms. No direct relationship between water temperature and ebullition rate was observed, indicating that the temperature within the sediment responds only slowly to water temperature changes. The high degree of synchronization (Fig. 7) and the observation that most of the gas was released during high-variability periods of hydrostatic pressure reveal the importance of the forcing regime for the temporal pattern of bubble release. In the case of the River Saar, physical forcing mechanisms control the temporal dynamics of ebullition on short timescales.

4.2 Forcing mechanisms

The ebullition rates during the daytime were significantly higher compared with the nighttime ebullition rates. At the Saar, there is no illumination of the sediment and therefore no warming of the sediment except by direct heat exchange between the water and sediment, and we recorded no daily pattern in the temperature except from 16 to 25 October 2012. Since temperatures within the sediment change over longer periods it can be assumed that there is only minor variation in the CH_4 production between day- and night-time caused by temperature changes. Hence, it is likely that there are other mechanisms that are responsible for the large temporal variability in ebullition rates.

The observation that the majority of large ebullition events matched clearly with pressure reductions due to ship locking and ship passages fits the diurnal pattern of ebullition. During the day, intensive locking and shipping activity dominate pressure fluctuations (Maeck and Lorke, 2013), while at night ship traffic decreased strongly and the variability in pressure also decreased. Lorke et al. (2012) observed a similar pattern for the flux of oxygen through the sediment–water interface and found that shipping and ship lock activity enhance oxygen flux by a factor of 2. The finding that pressure
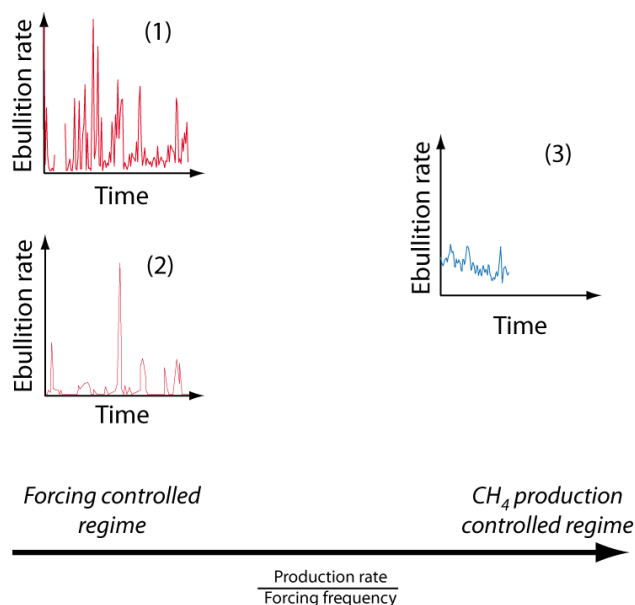
Figure 9. Conceptual framework for characterizing temporal variability of ebullition in aquatic systems differing in the relation between CH_4 production rates and forcing frequency of relevant trigger mechanisms for ebullition. All examples show ebullition rates (6-hour average) over a period of 4 weeks, except for (3), which refers to a period of 2 weeks. Example (1) shows the measured data from this study (Saar, ABT-1, January 2013), example (2) shows measurements from the Upper Mystic Lake (25 m site, October) taken from Varadharajan et al. (2012) and example (3) shows measured data from the River Main, Germany (Krotzenburg Dam, September 2012).

changes can act as a trigger is consistent with the results of other studies (Chanton et al. 1989; Joyce and Jewell, 2003; Varadharajan and Hemond, 2012). However, not all pressure reductions, e.g., by negative surges, showed a response in the ebullition rate. This may be due to the history of bubble release. If many bubbles were previously released the storage of free gas within the sediment may be smaller; therefore, even with an increase in gas volume due to pressure reduction the buoyancy of the gas may not be sufficient to cause bubble release. That the amount of free gas stored within a matrix can change was already shown for floating sediment mats in peatland (Fechner-Levy and Hemond, 1996) ship lock.

The passage of ships associated with different types of surface waves affected ebullition (Fig. 8c). However, ships can cause very different pressure changes and wave characteristics at the sampling site depending on the type of ship, its speed, the actual pathway of the ship track and the direction of the slipstream (Hofmann et al., 2008a). Therefore, the passage of ships can but will not always trigger ebullition. The example shown in Fig. 8c demonstrates that several ship passages had a strong effect on ebullition at ABT-1, but nearly no effect for the other two ABTs. This can result from the location of the ABTs and the morphology of the different sites.

While ships passed closer to ABT-1, ABT-2 and ABT-3 were further away from the main shipping channel and closer to the shore. Propagating diverging ship waves attenuate with travel length (Kundu and Cohen, 2008), but since ABT-2 and ABT-3 were closer than 80 m to the passing ships (ABT-1 is directly on the border of the shipping channel) the attenuation is of minor importance; therefore, the ship waves must have also been present at the locations of ABT-2 and ABT-3. Additionally, the shallower water depths at ABT-2 and ABT-3 should have led to proportionally stronger pressure changes due to bypassing waves compared to ABT-1. The missing gas release at ABT-2 and ABT-3 indicates that at ABT-1 the ebullition was not triggered by diverging surface waves, but rather by other processes in the vicinity of the ship, e.g., draft-induced pressure changes. However, we observed visually during our field campaigns that gas bubbles were released massively following the passage of large ship waves, but only in the more shallow areas (< 2 m water depth). Since the pressure signal caused by surface waves decreases with increasing depth and decreasing wave length (Kundu and Cohen, 2008), short waves, e.g., wind-induced or diverging ship waves, change the pressure at the sediment surface only in shallow regions, while long waves, e.g., surges, also affect the pressure in deeper areas.

Negative surges with a decrease in pressure showed stronger effects on ebullition compared to positive surges, which increase the pressure temporarily. Since the passage of both surges is associated with similar changes in current velocity (Maeck and Lorke, 2013), the effect of shear stress and pressure change on ebullition rates can be discriminated. Negative surges reduce the pressure, while positive surges increase the pressure. Significantly more large ebullition events co-occurred with negative surges, which indicates that the effects of pressure changes were stronger compared to shear stress (Fig. 8b, results section).

Sinking water level can also be a trigger for bubble release (Fig. 8a), but in the case of the River Saar this effect was of minor importance. Temporal changes in storage height may be much more important for systems with strong changes in water level, e.g., caused by hydropower peaking (Zohary and Ostrovsky, 2011).

The timescale of the relevant forcing mechanisms is on the order of seconds (ship waves), minutes (surges) and hours (sinking water level). Often, multiple occurrences of the individual mechanisms, e.g., during periods of intensive ship traffic, led to pronounced pressure fluctuations that caused gas venting from the sediments. We observed periods over which the forcing mechanisms are constantly active (periods of high variability in hydrostatic pressure), e.g., during the day, and periods of negligible forcing and lower ebullition rates (i.e., during the night). Since CH_4 production is continuously ongoing, forcing decouples production and gas release. The sediment therefore acts as a storage system for free gas, which further emphasizes the importance of forcing mechanisms for the temporal dynamics of gas release.

5 Implications

5.1 Timescale of forcing in other aquatic systems

The temporal dynamics of forcing mechanisms can be expected to differ among different aquatic systems. In lakes for example, water level changes are often caused by changes in the inflow of rivers on a timescale of days to weeks (Hofmann et al., 2008b; Jöhnk et al., 2004; Wilcox et al., 2007). In large lakes that have sufficient fetch length for wind energy input, seiches and propagating surface waves can generate short-term pressure fluctuations (Hamblin and Hollan, 1978). In lakes with limited fetch length, atmospheric and hydrostatic pressure changes have been demonstrated to trigger ebullition rates (Varadharajan and Hemond, 2012). In reservoirs, the inflow of water and the operation of dams are important, since pressure is predominantly controlled by the water level. In these systems water level drawdown can trigger ebullition, but wind speed may also affect gas venting (Joyce and Jewell, 2003). Ebullition rates in tidal systems were shown to be controlled by the tidal rise and fall of the water level (Boles et al., 2001). In general, many inland waters are exposed to periodically occurring forcing mechanisms with associated periods similar to those observed at the Saar.

The temporal pattern of ebullition from cohesive sediments is governed by two major factors: the production rate of CH_4 (approximated here by using the sedimentation rate as a proxy) and the timescale of forcing of sufficient magnitude (Fig. 9) to release bubbles. Ultimately, the ratio between the CH_4 production rate and the forcing frequency is the parameter that controls the temporal pattern of ebullition. Short-term (high-frequency) forcing in combination with high CH_4 production leads to the pattern observed within this study (Fig. 9-1) characterized by strongly variable ebullition rates on short timescales, but relatively constant fluxes after averaging over several days. Sites of lower CH_4 production that experience long-term (low-frequency) forcing mechanisms will release bubbles mainly during times of significant forcing, e.g., during water level reduction (Fig. 9-2), as observed by Varadharajan et al. (2012). Ultimately, the ratio of forcing frequency to CH_4 production rate will be on the same order of magnitude for both examples (as seen in Fig. 9-1 and 9-2); therefore, the ebullition variability and the resulting temporal pattern are predominantly controlled by forcing mechanisms. In contrast to forcing controlled regimes, highly productive systems exposed to long-term forcing may release bubbles more consistently following the rate of CH_4 production al illustrated in Figs. 9-3 with data from another German impoundment (the River Main at the Krotzenburg dam) that were collected with the same instrumentation and analyzed with the same methods as in this study. This site was located on the side upstream of the dam, where no ships can pass by, and since the River Main has a much larger cross-sectional area and a higher

discharge, ship lock-induced surges will not significantly affect the hydrostatic pressure at this site. Therefore, the ebullition rate may vary only little, but enhanced ebullition can occur during strong forcing periods, e.g., during periods of decreasing atmospheric pressure. This is an example of a CH_4 production-controlled regime. To verify this conceptual framework, which provides a useful a priori estimate of the temporal variability of CH_4 ebullition in aquatic systems, more high-resolution long-term ebullition data of different sites in combination with measurement of forcing parameters are necessary.

5.2 Implications for sampling intervals and duration

The recently developed guidelines for measuring greenhouse gas emissions from reservoirs (UNESCO/IHA 2011) recommend performing ebullition measurements over a period of at least 24 hours. In the River Saar, we observed a daily pattern with higher fluxes during the day, when ship locking and ship traffic induce water level fluctuations. During the night when ship traffic decreased, the water level fluctuations decreased and the ebullition rate was lower. Therefore, it is necessary to sample day and night. However, since forcing can be of varying magnitudes, the daily ebullition rate varied strongly and therefore, in the River Saar, ebullition measurements over 24 hours are not representative of longer periods (Fig. 6).

To determine the period of representative measurement, the variability in the ebullition rate itself is not the most important factor but rather the time span between episodes of strong gas release ("bubbling episodes"). For accurate extrapolation of short-term measurements to longer periods, it is necessary to measure over periods that cover the timescale of the bubbling episodes several times, since there is variability between the episodes (Fig. 5) (Varadharajan and Hemond, 2012). A representative measurement period at the Saar has to cover more than 10 days (indicated by the median in Fig. 8). In aquatic systems with longer periods between bubbling episodes, representative sampling periods will be much longer.

Our results show that short-term measurements are likely to underestimate the ebullition rate significantly, as illustrated by the median flux in Fig. 6 consistently remaining below 50 % of the monthly mean flux at shorter timescales. In contrast, if measurements are mainly performed during day time, ebullition rates are likely to be overestimated because some forcing mechanisms, whether naturally occurring such as wind or anthropogenically induced such as ship waves, are more likely to occur during the day. If measurements are performed during randomly chosen periods of 24 hr or shorter, the chance to underestimate ebullition rates by over 50 % is large (an average median of 54 % underestimation at 24 hr in Fig. 6).

Based on these findings, a representative sampling interval for forcing controlled ebullition regimes should at least cover several times the forcing mechanism timescale. Hence,

in systems with strong anthropogenic pressure changes like navigation channels, the interval should be at least 10 days, and for systems where natural forcing dominates, ebullition should be measured continuously because the timescale of atmospheric hydrostatic pressure changes is longer. Investigating hydrostatic pressure changes will help to identify the forcing timescale at work. Shorter sampling intervals are likely representative in systems with CH_4 production and minor physical forcing, but further studies are needed to support this.

Edited by: T. Del Sontro

References

Bastviken, D., Tranvik, L. J., Downing, J. A., Crill, P. M., and Enrich-Prast, A.: Freshwater methane emissions offset the continental carbon sink, Science, 331, 50, doi:10.1126/science.1196808, 2011.

Baulch, H. M., Dillon, P. J., Maranger, R., and Schiff, S. L.: Diffusive and ebullitive transport of methane and nitrous oxide from streams: are bubble-mediated fluxes important?, J. Geophys. Res.-Biogeo., 116, doi:10.1029/2011JG001656, 2011.

Becker, A., Kirchesch, V., Baumert, H. Z., Fischer, H., and Schöl, A.: Modelling the effects of thermal stratification on the oxygen budget of an impounded river, River Res. Appl., 26, 572–588, doi:10.1002/rra.1260, 2010.

Boles, J., Clark, J., Leifer, I., and Washburn, L.: Temporal variation in natural methane seep rate due to tides, Coal Oil Point area, California, J. Geophys. Res.-Oceans, 106, 27077–27086, doi:10.1029/2000JC000774, 2001.

Boudreau, B. P., Algar, C., Johnson, B. D., Croudace, I., Reed, A., Furukawa, Y., Dorgan, K. M., Jumars, P. A., Grader, A. S., and Gardiner, B. S.: Bubble growth and rise in soft sediments, Geology, 33, 517–520, doi:10.1130/G21259.1, 2005.

Chanton, J. P., Martens, C. S., and Kelley, C. A.: Gas transport from methane-saturated, tidal freshwater and wetland sediments, Limnol. Oceanogr., 34, 807–819, 1989.

Coulthard, T., Baird, A., Ramirez, J., and Waddington, J.: Methane dynamics in peat: importance of shallow peats and a novel reduced-complexity approach for modeling ebullition, carbon cycling in Northern Peatlands, Geophys. Monogr. Ser, 184, 173–185, doi:10.1029/2008GM000811, 2009.

DelSontro, T., McGinnis, D. F., Sobek, S., Ostrovsky, I., and Wehrli, B.: Extreme methane emissions from a Swiss hydropower reservoir: contribution from bubbling sediments, Environ. Sci. Technol., 44, 2419–2425, doi:10.1021/es9031369, 2010.

DelSontro, T., Kunz, M. J., Kempter, T., Wüest, A., Wehrli, B., and Senn, D. B.: Spatial heterogeneity of methane ebullition in a large tropical reservoir, Environ. Sci. Technol., 45, 9866–9873, doi:10.1021/es2005545, 2011.

Duc, N. T., Crill, P., and Bastviken, D.: Implications of temperature and sediment characteristics on methane formation and oxidation in lake sediments, Biogeochemistry, 100, 185–196, doi:10.1007/s10533-010-9415-8, 2010.

Emery, W. J. and Thomson, R. E.: Data Analysis Methods in Physical Oceanography, Elsevier Science Limited, Amsterdam, the Netherlands, 2001.

Fang, X. and Stefan, H. G.: Dynamics of heat exchange between sediment and water in a lake, Water Resour. Res., 32, 1719–1727, 1996.

Fang, X. and Stefan, H. G.: Temperature variability in lake sediments, Water Resour. Res., 34, 717–729, doi:10.1029/96WR00274, 1998.

Fechner-Levy, E. and Hemond, H.: Trapped methane volume and potential effects on methane ebullition in a northern peatland, Limnol. Oceanogr., 41, 1375–1383, 1996.

Forster, P., Ramaswamy, V., Artaxo, P., Berntsen, T., Betts, R., Fahey, D. W., Haywood, J., Lean, J., Lowe, D. C., Myhre, G., Nganga, J., Prinn, R., Raga, G., Schulz, M., and Van Dorland, R.: Changes in Atmospheric Constituents and in Radiative Forcing, in: Climate Change, The Physical Science Basis, Contribution of Working Group I to the Fourth Assessment Report of the Intergovernmental Panel on Climate Change, edited by: Solomon, S., Qin, D., Manning, M., Chen, Z., Marquis, M., Averyt, K. B., Tignor, M., and Miller, H. L., Cambridge University Press, Cambridge, United Kingdom and New York, NY, USA, 2007.

Goodrich, J. P., Varner, R. K., Frolking, S., Duncan, B. N., and Crill, P. M.: High-frequency measurements of methane ebullition over a growing season at a temperate peatland site, Geophys. Res. Lett., 38, doi:10.1029/2011GL046915, 2011.

Hamblin, P. F. and Hollan, E.: On the gravitational seiches of Lake Constance and their generation, Schweiz. Z. Hydrol., 40, 119–154, doi:10.1007/BF02502376, 1978.

Hofmann, H., Lorke, A., and Peeters, F.: The relative importance of wind and ship waves in the littoral zone of a large lake, Limnol. Oceanogr., 53, 368, doi:10.4319/lo.2008.53.1.0368, 2008a.

Hofmann, H., Lorke, A., and Peeters, F.: Temporal and spatial scales of water level fluctuations in lakes and their ecological implications, Hydrobiol., 613, 85–96, doi:10.1007/s10750-008-9474-1, 2008b.

Hofmann, H., Federwisch, L., and Peeters, F.: Wave-induced release of methane: littoral zones as a source of methane in lakes, Limnol. Oceanogr., 55, 1990–2000, doi:10.4319/lo.2010.55.5.1990, 2010.

Jöhnk, K. D., Straile, D., and Ostendorp, W.: Water level variability and trends in Lake Constance in the light of the 1999 centennial

flood, Limnologica-Ecology and Management of Inland Waters, 34, 15–21, doi:10.1016/S0075-9511(04)80017-3, 2004.

Johnson, B. D., Boudreau, B. P., Gardiner, B. S., and Maass, R.: Mechanical response of sediments to bubble growth, Mar. Geol., 187, 347–363, doi:10.1016/S0025-3227(02)00383-3, 2002.

Joyce, J. and Jewell, P. W.: Physical controls on methane ebullition from reservoirs and lakes, Environ. Eng. Geosci., 9, 167–178, doi:10.2113/9.2.167, 2003.

Kiene, R. P.: Production and consumption of methane in aquatic systems. Microbial production and consumption of greenhouse gases: Methane, nitrogen oxides and halomethanes, American Society for Microbiology, 111–146, 1991.

Kundu, P. K. and Cohen, I. M.: Fluid Mechanics, 4th edn., Elsevier Academic Press, Burlington, USA, 2008.

Leifer, I. and Patro, R. K.: The bubble mechanism for methane transport from the shallow sea bed to the surface: a review and sensitivity study, Cont. Shelf Res., 22, 2409–2428, doi:10.1016/S0278-4343(02)00065-1, 2002.

Liikanen, A. and Martikainen, P. J.: Effect of ammonium and oxygen on methane and nitrous oxide fluxes across sediment–water interface in a eutrophic lake, Chemosphere, 52, 1287–1293, doi:10.1016/S0045-6535(03)00224-8, 2003.

Lorke, A., McGinnis, D. F., Maeck, A., and Fischer, H.: Effects of ship locking on sediment oxygen uptake in impounded rivers, Water Resour. Res., 48, WR012514, doi:10.1029/2012WR012483, 2012.

Maeck, A. and Lorke, A.: Ship-lock induced surges in an impounded river and their impact on subdaily flow velocity variation, River Res. Appl., doi:10.1002/rra.2648, 2013.

Maeck, A., DelSontro, T., McGinnis, D. F., Fischer, H., Flury, S., Schmidt, M., Fietzek, P., and Lorke, A.: Sediment trapping by dams creates methane emission hot spots, Environ. Sci. Technol., 47, 8130–8137, doi:10.1021/es4003907, 2013.

McGinnis, D., Greinert, J., Artemov, Y., Beaubien, S., and Wüest, A.: Fate of rising methane bubbles in stratified waters: how much methane reaches the atmosphere?, J. Geophys. Res.-Oceans, 111, C09007, 8130–8137, doi:10.1029/2005JC003183, 2006.

Scandella, B. P., Varadharajan, C., Hemond, H. F., Ruppel, C. and Juanes, R.: A conduit dilation model of methane venting from lake sediments, Geophys. Res. Lett., 38, L06408, doi:10.1029/2011GL046768, 2011.

Schöl, A.: Die Saar – Auswirkungen der Stauregelung auf den Sauerstoffhaushalt in einem abflussarmen Mittelgebirgsfluss, in: Staugeregelte Flüsse in Deutschland, edited by: Kinzelbach, F. G., Ragnar, Stuttgart, Germany, 2006.

Segers, R.: Methane production and methane consumption: a review of processes underlying wetland methane fluxes, Biogeochemistry, 41, 23–51, doi:10.1023/A:1005929032764, 1998.

Sobek, S., DelSontro, T., Wongfun, N., and Wehrli, B.: Extreme organic carbon burial fuels intense methane bubbling in a temperate reservoir, Geophys. Res. Lett., 39, L01401, doi:10.1029/2011GL050144, 2012.

UNESCO/IHA: GHG Measurement Guidelines for Freshwater Reservoirs, edited by: Goldenfum, J. A., UNESCO, IHA, 2010.

USACE: Hydraulic design – surges in canals – change 1, in: Engineering and Design, US Army Corps of Engineering, Washington, DC, USA, 1–15, 1949.

Varadharajan C., Hermosillo R., and Hemond H. F.: A low-cost automated trap to measure bubbling gas fluxes, Limnol. Oceanogr. Meth., 8, 363–375, doi:10.4319/lom.2010.8.363, 2010

Varadharajan, C. and Hemond, H. F.: Time-series analysis of high-resolution ebullition fluxes from a stratified, freshwater lake, J. Geophys. Res.-Biogeo., 117, G02004, doi:10.1029/2011JG001866, 2012.

Venkiteswaran, J. J., Schiff, S. L., St. Louis, V. L., Matthews, C. J., Boudreau, N. M., Joyce, E. M., Beaty, K. G., and Bodaly, R. A.: Processes affecting greenhouse gas production in experimental boreal reservoirs, Global Biogeochem. Cy., 27, 1–11, doi:10.1002/gbc.20046, 2013.

Wik M., Crill, P. M., Varner, R. K., and Bastviken, D.: Multiyear measurements of ebullitive methane flux from three subarctic lakes, J. Geophys. Res. Biogeo., 118, 1307–1321, doi:10.1002/jgrg.20103, 2013

Wilcox, D. A., Thompson, T. A., Booth, R. K., and Nicholas, J.: Lake-level variability and water availability in the Great Lakes, US Geological Survey, 2007.

Zohary, T. and Ostrovsky, I.: Do water level fluctuations matter?, Inland Waters, 1, 47–59, 2011.